CODEE Journal

Volume 9 Article 12

5-12-2012

A Simple Charged Three-Body Problem

Jaie Woodard

James Walsh

A Simple Charged Three-Body Problem

Jaie Woodard
Biophysics Program, Harvard University

James Walsh
Department of Mathematics, Oberlin College

Dedicated to Paul Blanchard on the occasion of his sixtieth birthday.

Keywords: oscillator, Poincaré map, bifurcation, basin
Manuscript received on January 10, 2012; published on May 12, 2012.

Abstract: The dynamics of a simple model of three charged bodies interacting under an inverse square electrostatic force is presented. The model may be viewed as an alternative to the pendulum, the standard model of a periodically forced and damped nonlinear oscillator.

1 Introduction

Does your department offer a follow-up to the sophomore-level ODE course? Perhaps an upper-level ODE or PDE course, or an introductory dynamical systems course? The second author still remembers and is, indeed, fortunate to have taken just such a course from Paul Blanchard at Boston University many years ago.

There is but one mathematics course devoted to the study of ODEs at Oberlin College, and that is the sophomore-level course. Walsh does teach an upper-level *discrete* dynamical systems course (Math 302), which was taken recently by the first author. But what does a discrete dynamical systems course have to do with the study and teaching of ODEs?

The connection comes from the requirement that students complete independent projects in Math 302, either individually or in small groups, for which the expectations are high. It is via these research projects that the study of ODEs arises, most often in the context of mathematical modeling. In this article the model Woodard created and analyzed for her project is presented, both for its intrinsic interest and as a simple alternative to the the pendulum, often viewed as the standard model of a periodically forced and damped nonlinear oscillator [7]. The exact interplay of gravitation, forcing, and damping is arguably difficult to visualize, however, when seeking an intuitive understanding of just why the pendulum behaves chaotically for certain parameter regimes. (See, for example, the animation at `http://www.myphysicslab.com/pendulum2.html`.)

After introducing the model, a variety of simulations and animations will be presented, all of which were executed in *Mathematica*. More recent versions of this computer algebra system clearly have an increased facility when it comes to performing computer experiments related to ODEs.

2 The Model ODE

Consider a charged particle p_0 of mass m, constrained to move along a straight line, which we take to be the x-axis. Place two charged particles p_1 and p_2 on the y-axis. Particle p_2, with position fixed for all time at a distance d_2 below the x-axis, exerts an attractive force on p_0, while p_1 exerts a repulsive force on p_0. Assume that p_1 oscillates vertically over time, so that its distance above the x-axis is given by $p_1(t) = d_1 + A\cos t,\ A > 0$ (see Figure 1). We assume $A < d_1$ throughout so that p_1 never collides with p_0.

The magnitude of the force $\mathbf{F}_i$ exerted on p_0 by particle p_i is assumed to be inversely proportional to the the square of the distance r_i between p_0 and p_i, $i = 1, 2$. In addition, we assume the magnitude of $\mathbf{F}_2$ is greater than the magnitude of $\mathbf{F}_1$ when p_1 and p_2 are equidistant from p_0. We thus have a model of a simple 3-body problem, one in which the force between bodies is electrostatic rather than gravitational. For a more sophisticated treatment of a charged 3-body model, see [2].

Let $x = x(t)$ denote the position of particle p_0 as a function of time. The goal is to understand the behavior of $x(t)$ as time varies and as initial conditions and parameters change. This requires, of course, that we first derive the model ODE.

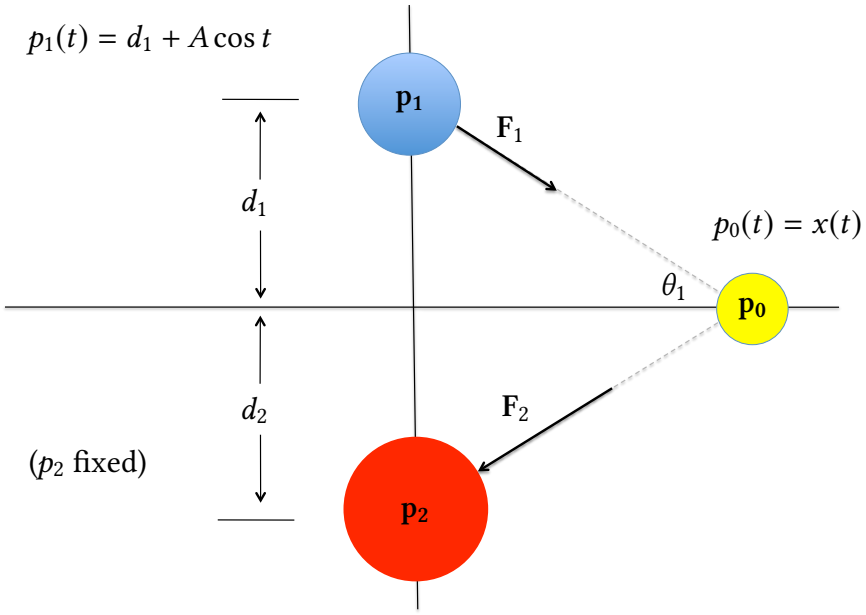

Figure 1: The model set-up

By assumption, we have

$$\|\mathbf{F}_1\| = \frac{k_1}{r_1^2} = \frac{k_1}{(d_1 + A\cos t)^2 + x^2} \text{ and } \|\mathbf{F}_2\| = \frac{k_2}{r_2^2} = \frac{k_2}{d_2^2 + x^2}, \quad 0 < k_1 < k_2.$$

The sum of the horizontal components of $\mathbf{F}_1$ and $\mathbf{F}_2$ is then

$$\begin{aligned} F_x &= \|\mathbf{F}_1\| \cos\theta_1 + \|\mathbf{F}_2\| \cos\theta_2 \\ &= \frac{k_1 x}{((d_1 + A\cos t)^2 + x^2)^{3/2}} - \frac{k_2 x}{(d_2^2 + x^2)^{3/2}}. \end{aligned}$$

Assuming that damping is proportional to velocity we have, via Newton's Second Law, $F_x - b'\dot{x} = m\ddot{x},\ b' \geq 0$. Letting $q_i = k_i/m,\ i = 1, 2$, and $b = b'/m$, we have

$$\ddot{x} = \frac{q_1 x}{((d_1 + A\cos t)^2 + x^2)^{3/2}} - \frac{q_2 x}{(d_2^2 + x^2)^{3/2}} - b\dot{x}, \quad 0 \leq b, \quad 0 < q_1 < q_2, \tag{2.1}$$

a second-order nonlinear ODE. We thus wish to understand the behavior of solutions to equation (2.1).

The analysis to follow is interspersed with animations created with *Mathematica*. Animation 1, for example, presents a solution which converges to a periodic solution comprised of three "bumps" to the right and three bumps to the left. With regard to animations, we agree with Paul Blanchard, who wrote [3]:

> If a picture is worth 1000 words, then a good animation is like a classic short story—a simple tale simply told. Animations are particularly effective in the teaching of mathematics because motion is often fundamental to the concept at hand, and a well designed animation is usually an excellent way to introduce such a concept.

We found that using *Mathematica* as an investigative tool provided great insight into the dynamics of this model.

3 The case of no damping and no forcing

Let's assume, for simplicity, that $d_1 = d_2 = d$ for the remainder of this article. Setting $A = b = 0$ in equation (2.1) then yields

$$\ddot{x} = -\frac{(q_2 - q_1)x}{(d^2 + x^2)^{3/2}}. \tag{3.1}$$

Note that for very small x, equation (3.1) is approximated by

$$\ddot{x} = -\omega^2 x, \quad \omega^2 = \frac{q_2 - q_1}{d^3}, \tag{3.2}$$

as x^2 will be much smaller than x in this case. Equation (3.2) is easily recognizable as an equation for a harmonic oscillator, with general solution

$$x(t) = x_0 \cos \omega t + \frac{v_0}{\omega} \sin \omega t, \quad (x(0), \dot{x}(0)) = (x_0, v_0).$$

Solutions of equation (3.2) are plotted in the $(x, \dot{x})$-phase plane in Figure 2. (For this and all subsequent plots, we use the values $q_1 = 5$, $q_2 = 10$ and $d = 1.5$.)

What of solutions to equation (3.1)? Given the absence of damping and forcing at this point, one might expect conservation of energy to play a role.

To see that this is indeed the case, we first convert the second order equation (3.1) into a first order system, as on page 164 of Borrelli and Coleman [5]. Letting $v = v(t)$ denote the velocity $\dot{x}$ of p_0, equation (3.1) corresponds to the planar system

$$\dot{x} = v \tag{3.3a}$$

$$\dot{v} = -\frac{(q_2 - q_1)x}{(d^2 + x^2)^{3/2}}. \tag{3.3b}$$

Now letting $H(x, v) = v^2/2 - (q_2 - q_1)/\sqrt{d^2 + x^2}$, we note

$$\frac{\partial H}{\partial v} = v = \dot{x} \quad \text{and} \quad \frac{\partial H}{\partial x} = \frac{(q_2 - q_1)x}{(d^2 + x^2)^{3/2}} = -\dot{v}.$$

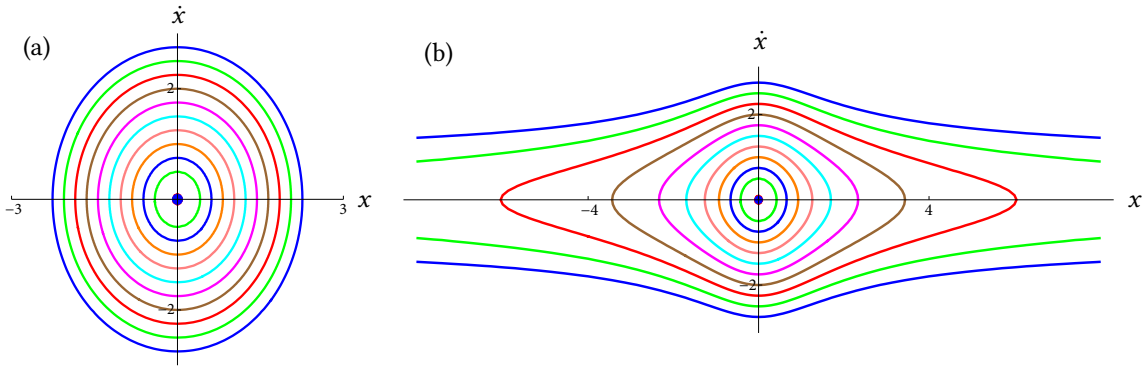

Figure 2: The case of no damping and no forcing. (a) The linear approximation, for small x, given by equation (3.2). (b) The phase plane for system (3.3).

Hence, if $(x(t), v(t))$ represents a solution curve of system (3.3), we have

$$\frac{d}{dt}H(x(t), v(t)) = \frac{\partial H}{\partial x}\frac{dx}{dt} + \frac{\partial H}{\partial v}\frac{dv}{dt} = -\dot{v}\dot{x} + \dot{x}\dot{v} = 0.$$

This implies the function H is constant along solutions to system (3.3), that is, solutions to system (3.3) lie on level sets of H (which level set depends on the initial condition). Such a function H is called a *Hamiltonian function* and, in applications to mechanics, often represents the total mechanical energy (see §5.3 in [4]).

Solutions to system (3.3) are plotted in Figure 2. Note how well solutions to equation (3.2) in the $(x, \dot{x})$-phase plane approximate solutions to system (3.3) near the origin.

If particle p_0 is placed on the positive x-axis and given a sufficiently strong push to the left, it will move monotonically to the left with $x(t) \to -\infty$ as $t \to \infty$. Using the Hamiltonian function H above, however, one can show that if p_0 is placed at initial position $(x(0), 0)$ (so that it starts from rest), its motion will be periodic. Two such $(t, x(t))$ solutions are plotted in Figure 3; also see Animation 2.

In this regard system (3.3) can be viewed as modeling a nonlinear oscillator. What happens if we first damp the system and then add periodic forcing?

4 The damped, unforced case

Setting $A = 0$ and $b > 0$ in equation (2.1), and letting $v = \dot{x}$ and $d_1 = d_2 = d$, yields the autonomous system

$$\dot{x} = v = f(x, v) \tag{4.1a}$$

$$\dot{v} = -\frac{(q_2 - q_1)x}{(d^2 + x^2)^{3/2}} - bv = g(x, v). \tag{4.1b}$$

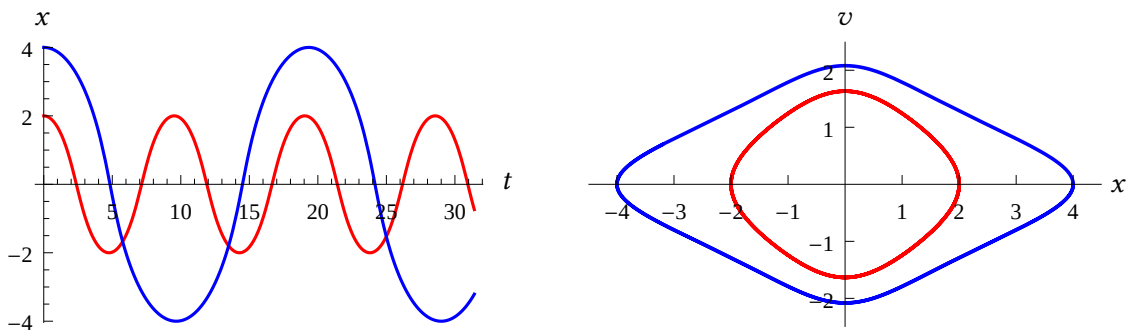

Figure 3: Two periodic solutions of system (3.3). *Red*: $(x(0), v(0)) = (2, 0)$. *Blue*: $(x(0), v(0)) = (4, 0)$.

Due to the damping term the system is now dissipative in the sense that it loses energy over time. We make this more precise shortly.

Note that $(x(t), v(t)) = (0, 0)$ is the sole equilibrium solution for system (4.1). To determine the nature of this equilibrium point we linearize the system at $(0, 0)$ (§8.2 in [5]). Computation of the Jacobian matrix J at $(0, 0)$ yields

$$J(0,0) = \left[\begin{array}{cc} \frac{\partial f}{\partial x} & \frac{\partial f}{\partial v} \\ \frac{\partial g}{\partial x} & \frac{\partial g}{\partial v} \end{array}\right]\Bigg|_{(0,0)} = \left[\begin{array}{cc} 0 & 1 \\ -a & -b \end{array}\right], \quad a = \frac{q_2 - q_1}{d^3} > 0, \quad b > 0.$$

The eigenvalues of the Jacobian matrix $J(0, 0)$ are $\lambda_\pm = \frac{1}{2}(-b \pm \sqrt{b^2 - 4a})$. Thus for small damping $(b^2 < 4(q_2 - q_1)/d^3)$, the eigenvalues are complex numbers with negative real part. Since the vector field $\mathbf{V} = (f, g)$ is twice continuously differentiable, this implies the origin is an asymptotic spiral sink (Theorem 8.2.1 in [5]). The oscillator is underdamped in this case (see Figure 4).

For larger values of b $(b^2 > 4(q_2 - q_1)/d^3)$, the eigenvalues of $J(0, 0)$ are distinct, real and negative (recall $a > 0$). Hence the phase plane for the linearized system has a sink at $(0, 0)$ with two "straight line" solutions (§3.2 in [4]). A typical solution to system (4.1) for these b-values is plotted in Figure 4; we see that the oscillator is overdamped.

It is natural to ask whether this stable long-term behavior will persist when particle p_1 begins to oscillate, applying a periodic force to p_0.

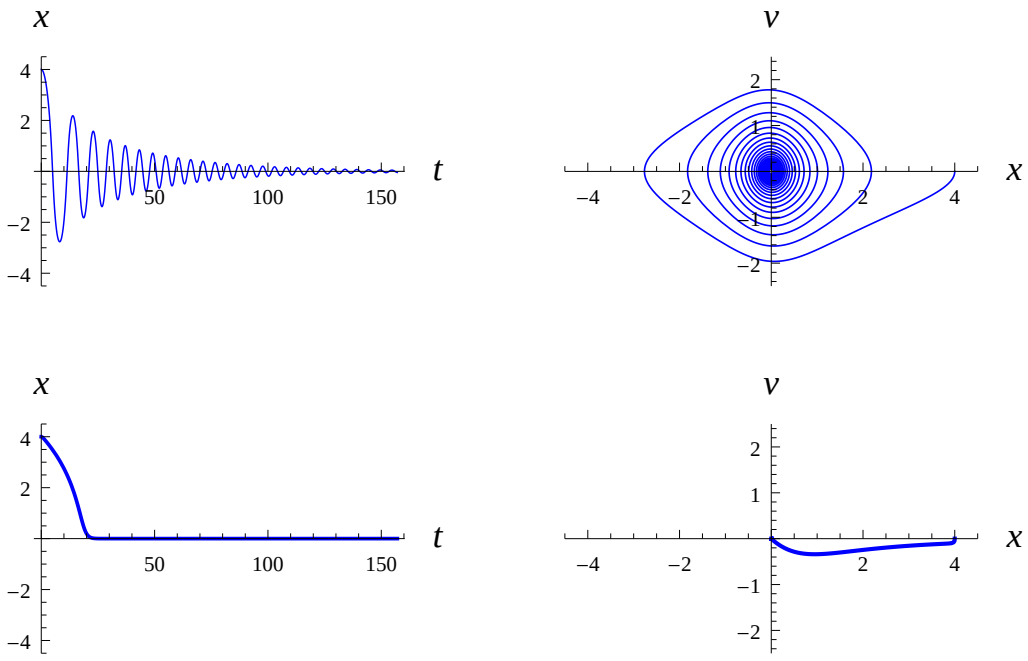

Figure 4: Two solutions to system (4.1), each with $(x(0), v(0)) = (4, 0)$. *Top*: $b = 0.05$ (underdamped). *Bottom*: $b = 2.5$ (overdamped).

5 Damping with forcing

We now consider the first-order system corresponding to equation (2.1):

$$\dot{x} = v \tag{5.1a}$$

$$\dot{v} = \frac{q_1 x}{((d + A\cos t)^2 + x^2)^{3/2}} - \frac{q_2 x}{(d^2 + x^2)^{3/2}} - bv. \tag{5.1b}$$

5.1 The Poincaré map

Solutions to the nonautonomous system (5.1) live in (x, v, t)-space. To reduce the dimension of this state space by one we turn to the *Poincaré*, or *first-return*, map associated with this system of ODEs. Given that the vector field in system (5.1) is periodic in t with period 2π, we will sample solutions at integer multiples of 2π. This yields a mapping $P = P_{A,b} : \mathbb{R}^2 \to \mathbb{R}^2$, which sends the point (x_0, v_0) to the value at time $t = 2\pi$ of the solution to system (5.1) having initial condition (x_0, v_0). That is, if $(x(t), v(t))$ is the solution with initial condition $(x(0), v(0)) = (x_0, v_0)$, then $P(x_0, v_0) = (x(2\pi), v(2\pi))$. We are thus sampling a given solution each time particle p_1 completes one oscillation.

Letting P^n denote the n-fold composition of P with itself, we have that $P^n(x_0, v_0) = (x(2\pi n), v(2\pi n))$ for $n \geq 1$. We thus iterate the Poincaré map P in the (x, v)-plane to deduce the qualitative long-term behavior of solutions to system (5.1) (see Figure 5 for an example in the case $b = 0$).

Note that $(x(t), v(t)) = (0, 0)$ is a solution of system (5.1) for all parameter values. This implies $(0, 0)$ is a *fixed point* of the Poincaré map, that is, $P(0, 0) = (0, 0)$ for all parameter values.

The dissipative nature of this model is a consequence of the damping. This is evidenced mathematically by the fact the Poincaré map contracts area in the plane each iterate for

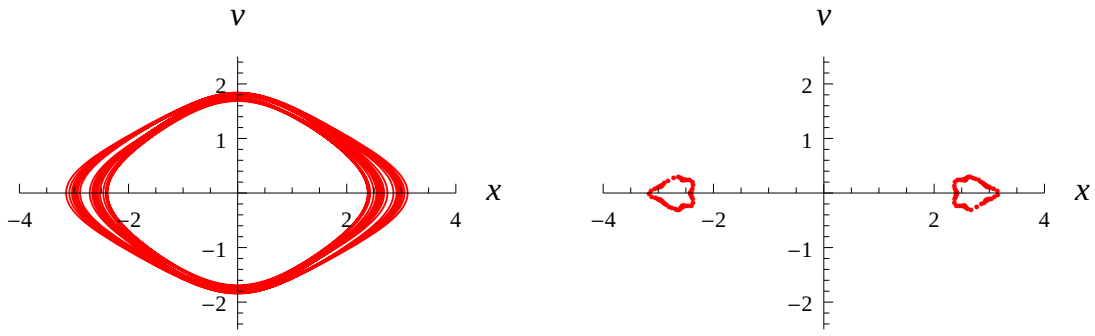

Figure 5: *Left*: The projection of a solution to system (5.1) onto the (x, v)-plane. *Right*: The corresponding Poincaré orbit. $(A = 0.11, b = 0, (x(0), v(0)) = (2.553, 0.2373))$

any $A > 0$ and $b > 0$. To see this, we convert system (5.1) into an autonomous system in 3-space:

$$\dot{x} = v = f(x, v, t) \tag{5.2a}$$

$$\dot{v} = \frac{q_1 x}{((d + A\cos t)^2 + x^2)^{3/2}} - \frac{q_2 x}{(d^2 + x^2)^{3/2}} - bv = g(x, v, t) \tag{5.2b}$$

$$\dot{t} = 1 = h(x, v, t) \tag{5.2c}$$

We then use Liouville's formula, as in §9.6 in [1]. To that end, let $M(t)$ denote the Jacobian of the vector field (f, g, h) evaluated along the solution to system (5.2) with initial value $(x_0, v_0, 0)$. Note that the trace of $M(t)$ is

$$\mathrm{Tr}(M(t)) = \frac{\partial f}{\partial x} + \frac{\partial g}{\partial v} + \frac{\partial h}{\partial t} = 0 - b - 0 = -b.$$

Liouville's formula then says the area contraction per iterate of P is given by

$$\exp\left(\int_0^{2\pi} \mathrm{Tr}(M(t))\, dt\right) = \exp\left(\int_0^{2\pi} -b\, dt\right) = e^{-2\pi b}.$$

This implies in particular that any fixed or periodic points of P must be of either attracting or saddle type. What else can be said concerning periodic points for the Poincaré map?

5.2 Bifurcations

In this section we fix the value $b = 2$ and increase the value of the amplitude A of the periodic forcing. We are interested in experimentally determining any changes in the long-term behavior of particle p_0 as a function of A. Recall that for $A = 0$ and $b > 0$, the origin $(0, 0)$ is a sink in the (x, v)-phase plane, so that $(0, 0)$ is an attracting fixed point for the Poincaré map in this case.

Plotted in Figure 6 are a variety of $(t, x(t))$ solution curves and corresponding Poincaré orbits for $b = 2$ and $A > 0$. Note that for A as large as 0.75, the solution still converges to the origin. Periodic behavior emerges, however, as A increases through 0.9. We note that discrete periodic orbits for the Poincaré map P correspond to continuous periodic solutions for system (5.1). The period-4 cycle illustrated in Figure 6 for $A = 0.9617$ is rendered in Animation 3.

The existence of periodic behavior as A varies strongly suggests that we execute the following computer experiment: Plot the long-term behavior of solutions (via Poincaré orbits) as a function of A in a *bifurcation diagram*.

Our approach is adapted from an algorithm in [8], and proceeds as follows. For a given value of A, select an initial condition near the fixed point $(0, 0)$. For definitiveness, we will set $(x(0), v(0)) = (0.1, 0)$. Sample the corresponding solution to ODE (5.1) at integer multiples of 2π, generating a list of position and velocity values for particle p_0. After discarding the first 100 points, compute the distance of each remaining point (x, v) from

the origin. For each of these distances r we the plot the point (A, r). Then select a new A-value and repeat.

We note this approach has certain drawbacks. For example, a period-2 cycle in which

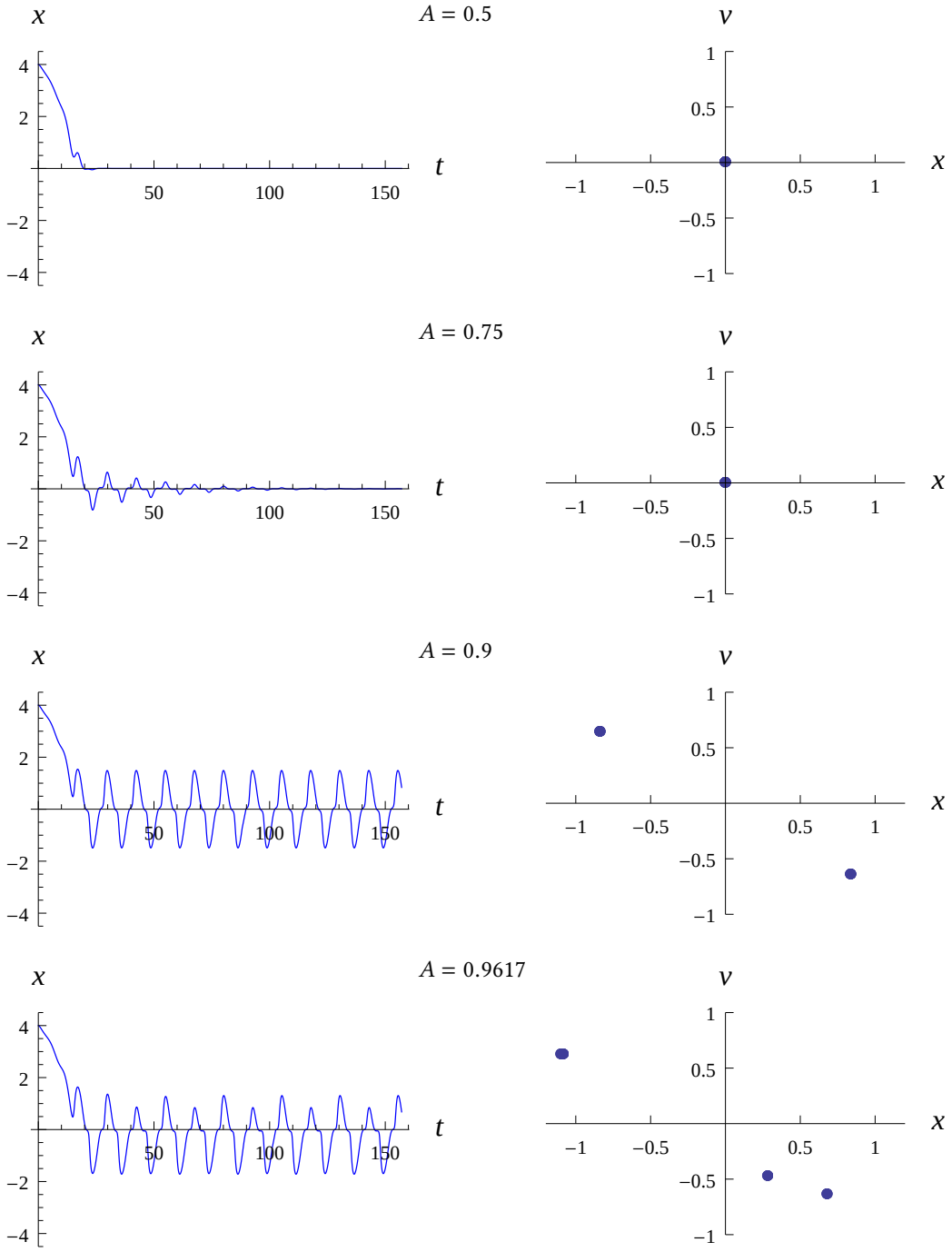

Figure 6: Solutions to system (5.1) with $b = 2$ and A varying as indicated. *Left*: $(t, x(t))$ plots. *Right*: Iterates 125 through 150 of the Poincaré map corresponding to the given solution.

both points are equidistant from the origin will yield but one point in the (A, r)-plane, rather than two. In addition, this algorithm finds at most one attracting periodic orbit, whereas more than one attracting cycle may be present for a given A-value. Nonetheless, this simple approach helps to elucidate the remarkably complicated behavior of particle p_0 as A increases.

Two views of the bifurcation diagram, each with $A < 1$, are presented in Figure 7. Note the striking similarity to the well-known bifurcation diagram for the logistic map $f_\lambda(x) = \lambda x(1-x)$ (§11.2 in [6]). As the amplitude of the periodic motion of particle p_1 increases from 0 to 1, the behavior of particle p_0 follows the period-doubling route to chaotic dynamics.

The small arrow embedded within Figure 7 points to a "period-6 window." The corresponding periodic orbit is shown in Figure 8.

It is relatively easy to see why the behavior of particle p_0 depends sensitively on initial conditions for certain parameter values. The force exerted by particle p_1 on p_0 is greatest when p_1 is closest to the origin (at t-values near $t_k = (2k+1)\pi$, k an integer). Recall that $d_1 = d = 1.5$ in all simulations. As A increases toward 1.5, p_1 exerts an ever greater force on p_0, particularly when t has a value near an odd multiple of π while p_0 is simultaneously near the origin. If p_0 is just to the right of the origin at a time near t_k, it will receive a large push to the right, while if it is just to the left, it will receive a large push to the left. This sensitivity to initial conditions is illustrated in Figure 9 and in Animation 4.

The interplay of the periodic forcing, gravity and damping, and the role these forces play in determining the model dynamics, is relatively easy to grasp in this setting.

5.3 Fractal basin boundaries

It is well known that basins of attraction of fixed and periodic points for the forced, damped pendulum have a fractal structure for certain parameter values ([7], §2.1 in [1]). We now show this also holds true in this simple charged 3-body model.

System (5.1) admits two attracting periodic orbits when $b = 2$ and $A = 1$, as indicated in Figure 10. The corresponding fixed points of the Poincaré map P lie at roughly $\ell_1 = (1.23, -0.6)$ and $\ell_2 = (-1.23, 0.6)$. We implement, via *Mathematica*, an algorithm outlined in [7] which generates the basins of attraction of ℓ_1 and ℓ_2 under P. Start by choosing a large grid of initial conditions. Compute the Poincaré orbit of each point in the grid, and color the initial condition blue or red, depending on whether the orbit limits on ℓ_1 or ℓ_2, respectively. The results are shown in Figure 11.

The behavior of p_0 for initial conditions near or on the common boundary of the two basins presented in Figure 11 is of particular interest. Let the symbol L correspond to a negative local minimum on the (t, x)-graph of a given solution (so a "bounce" to the left), and let R correspond to a positive local maximum (a bounce to the right). One can then assign strings (often called *symbol sequences*) of Ls and Rs to trajectories, as illustrated in Figure 12. (Animation 5 corresponds to the lower right solution in Figure 12.) The conjecture is that corresponding to any symbol string is an initial condition (x_0, v_0) on the basin boundary whose solution provides this exact string in terms of the sequence of bounces to the left and right. A proof of this conjecture would likely involve showing that the Poincaré map admits a Smale horseshoe, as in [7].

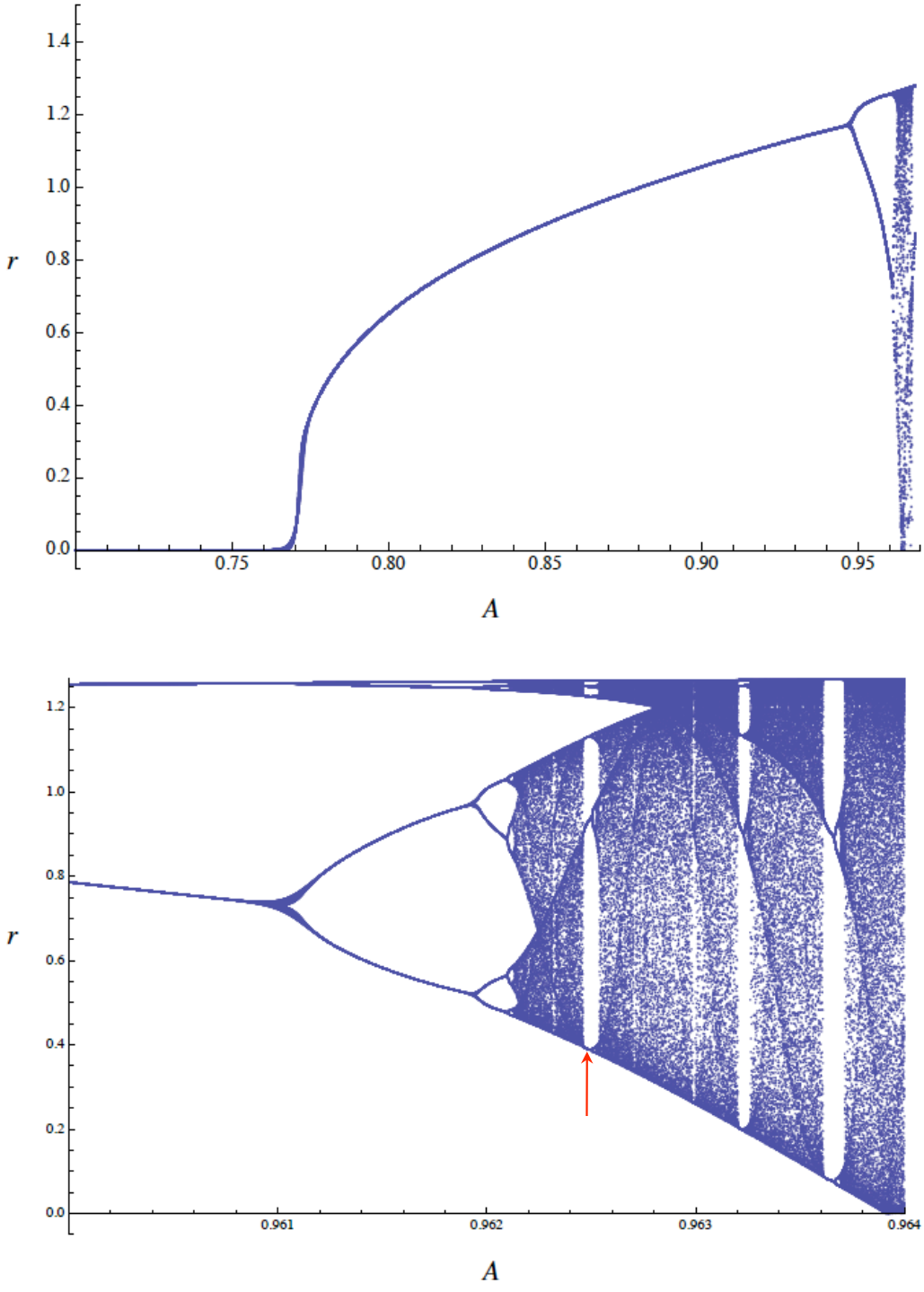

Figure 7: The bifurcation diagram for system (5.1) with $b = 2$ and A varying. *Top*: $0.7 \leq A < 1$. *Bottom*: $0.96 \leq A \leq 0.964$.

We note that if we fix $A = 1$ and weaken the damping $b < 2$, there appear to be b-values for which no attracting cycles exist. A single orbit of the Poincaré map when $A = 1$ and $b = 0.1$ is presented in Figure 13, which is similar in spirit to Figure 2.7 in [1].

Finally, if the periodic forcing remains but we remove all damping, a completely different story emerges. The analysis in this case requires the celebrated KAM theory, which we will present in a subsequent paper.

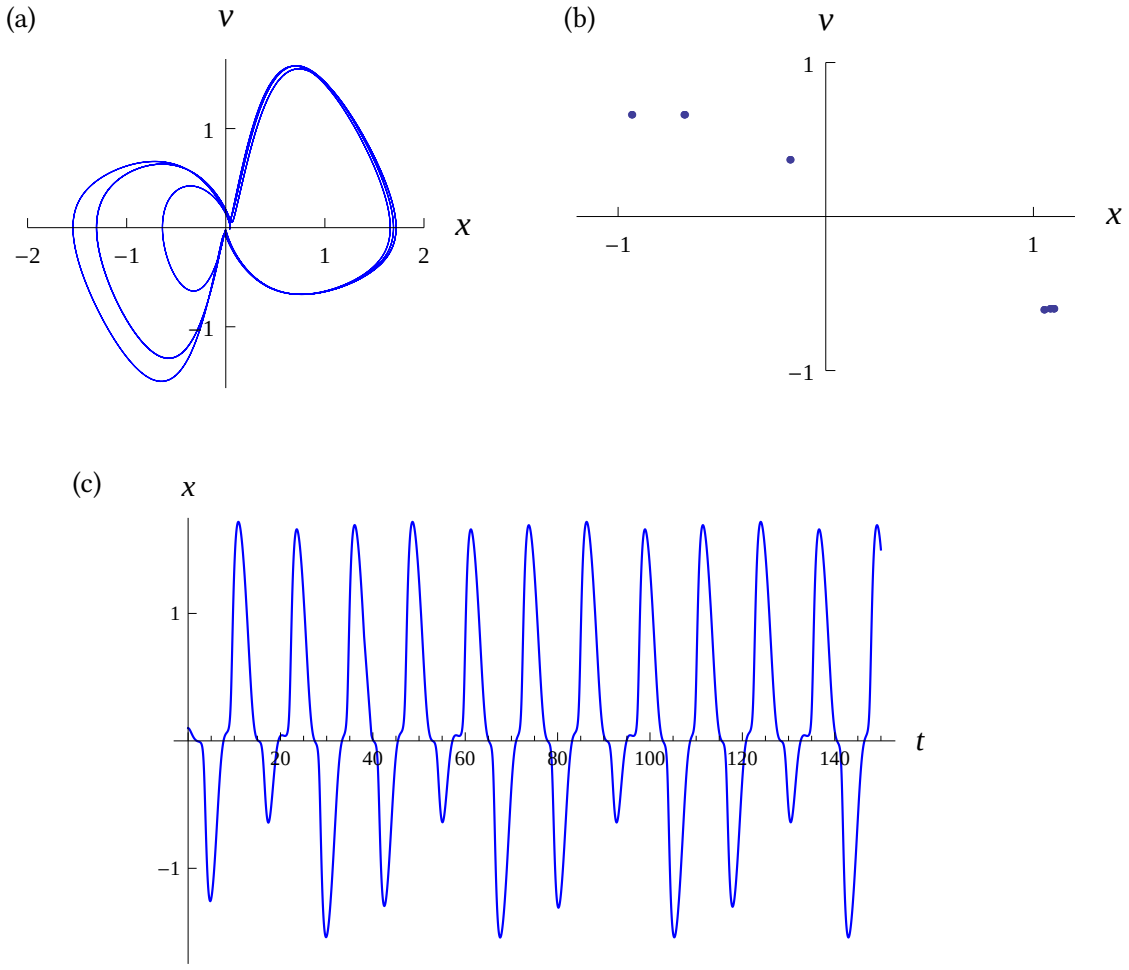

Figure 8: A periodic solution to system (5.1) corresponding to the position of the red arrow in Figure 7. (a) Projection onto the (x, v)-plane. (b) Iterates 125 through 150 of the Poincaré map corresponding to this solution. (c) The solution in (t, x)-space.

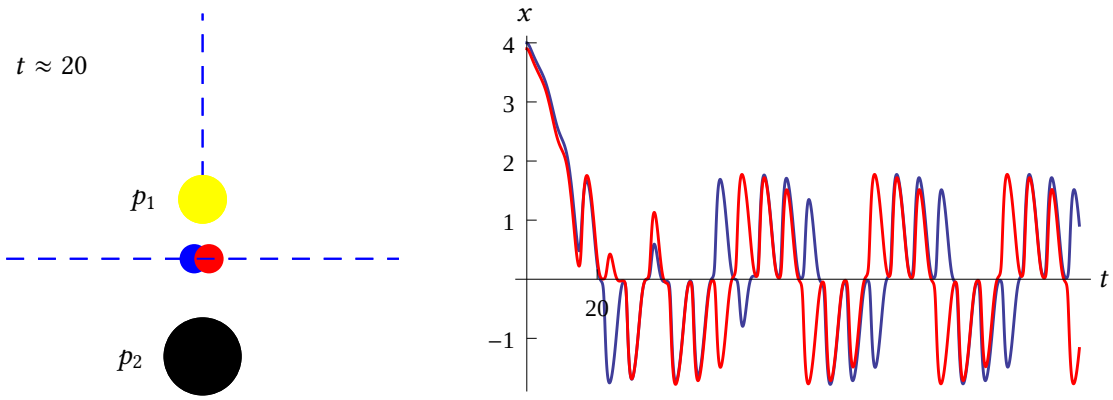

Figure 9: Sensitive dependence on initial conditions. *Blue*: $(x(0), v(0)) = (4, 0)$. *Red*: $(x(0), v(0)) = (3.9, 0)$. Near $t = 20$, particle p_1 pushes the red p_0 to the right, and the blue p_0 to the left.

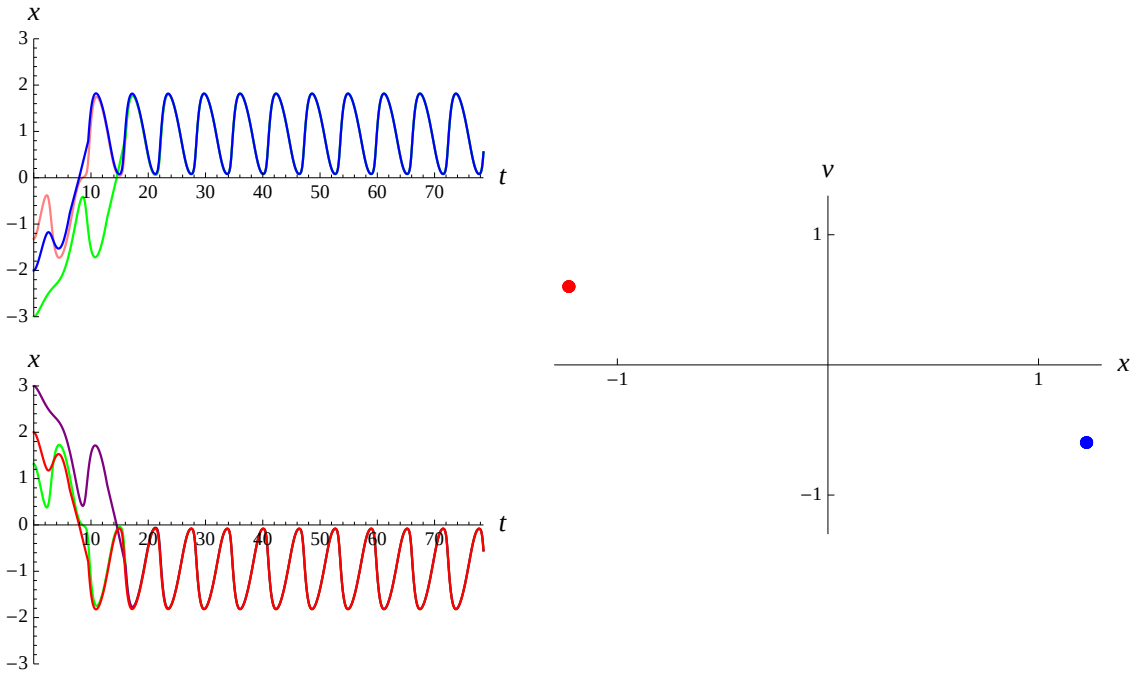

Figure 10: Two attracting cycles for $A = 1,\ b = 2$, and the corresponding fixed points for the Poincaré map.

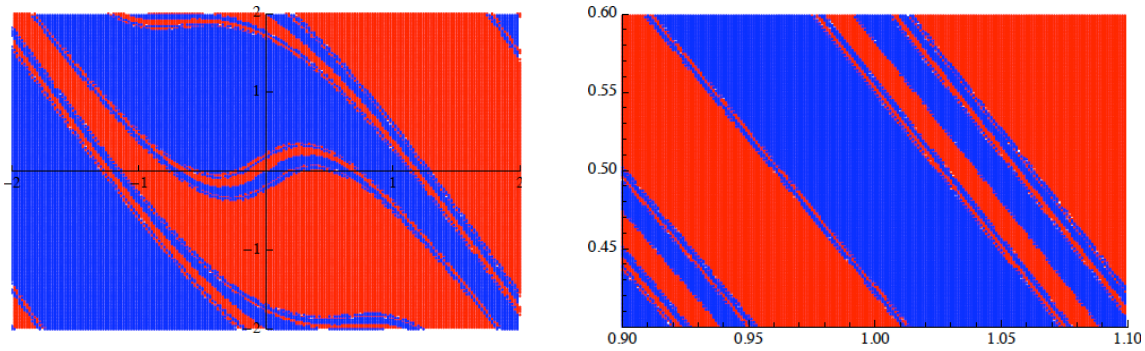

Figure 11: The basins of attraction for the blue and red fixed points shown in Figure 10. Zooming in on the common boundary would continue to produce ever finer striations of blue and red points.

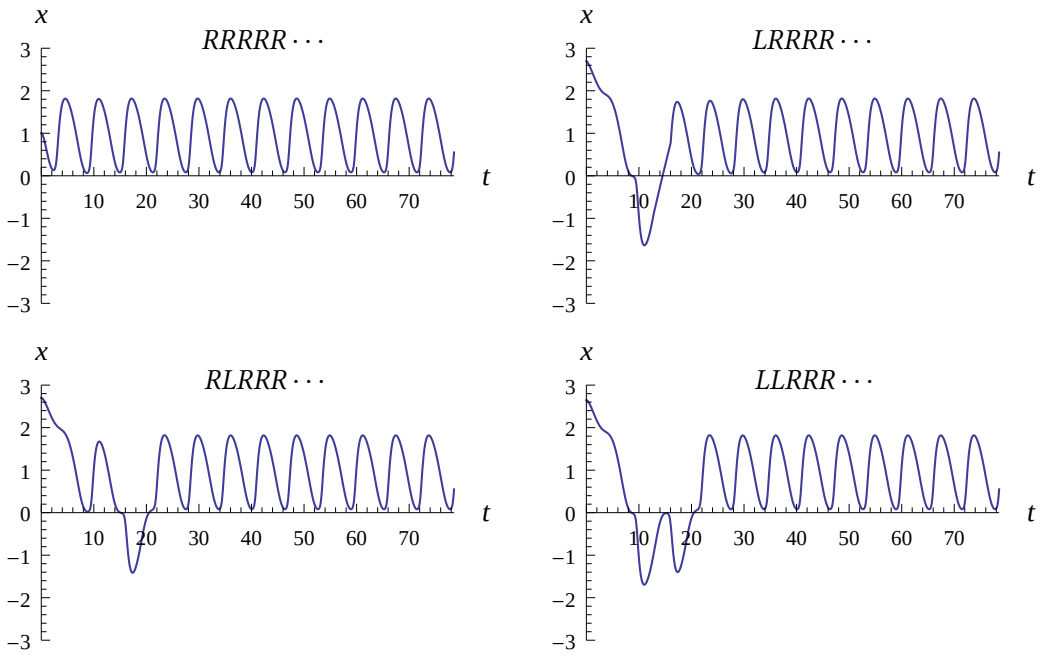

Figure 12: The assignment of symbol sequences to solutions to system (5.1) for $A = 1, b = 2$.

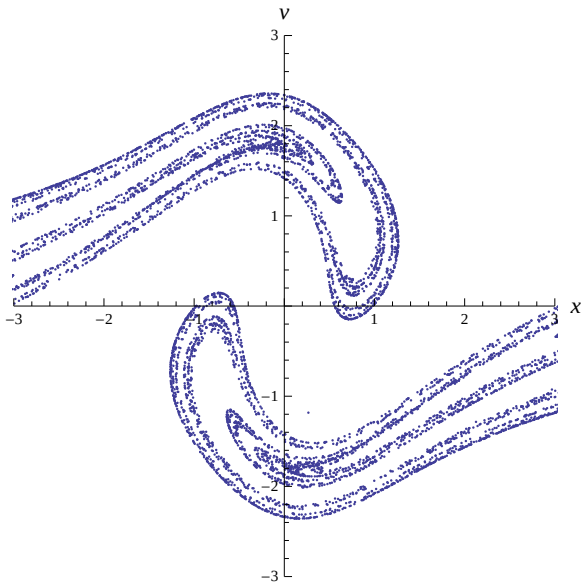

Figure 13: The Poincaré orbit of a single solution for $A = 1, b = 0.1$, and $(x(0), v(0)) = (0.5, 0)$. Other orbits also limit on this chaotic attractor.

6 Conclusion

The model presented in this article is a simple alternative to the forced and damped pendulum. While the interplay of the physical forces vis-à-vis the dynamics is more intuitive in Woodard's model, the motion of particle p_0 exhibits all of the behavior one finds in the pendulum model. A computer algebra system, such as *Mathematica*, can and should play an important role as students, in increasing numbers, create and investigate the behavior of new and intriguing mathematical models.

References

[1] Kathleen Alligood, Tim Sauer, and James Yorke. *Chaos An Introduction to Dynamical Systems*. Springer-Verlag, 1997.

[2] Pau Atela and Robert McLachlan. Global behavior of the charged isosceles three-body problem. *Internat. J. Bifur. Chaos Appl. Sci. Engrg.*, 4(4):865–884, 1994.

[3] Paul Blanchard. Easy animations, 2004. Web page resource accessible from http://math.bu.edu/people/paul/nsf_ccli_presentation_2004.html.

[4] Paul Blanchard, Robert Devaney, and G.R. Hall. *Differential Equations*. Thomson Brooks/Cole, 3rd edition, 2006.

[5] Robert Borrelli and Courtney Coleman. *Differential Equations: A Modeling Perspective*. Wiley, 2nd edition, 2004.

[6] Boris Hasselblatt and Anatole Katok. *A First Course in Dynamics with a Panorama of Recent Developments.* Cambridge University Press, 2002.

[7] John H. Hubbard. The forced damped pendulum: Chaos, complication and control. *The American Mathematical Monthly*, 106(8):741–758, 1999.

[8] Stephen Lynch. *Dynamical Systems with Applications using Mathematica.* Birkhäuser, 2007.